

Proton Nuclear Magnetic Resonance and Laser Photolysis Studies of Pyrene Derivatives in Aqueous and Micellar Solutions

M. Grätzel, K. Kalyanasundaram, and J. K. Thomas*

Contribution from the Department of Chemistry and Radiation Laboratory,¹ University of Notre Dame, Notre Dame, Indiana 46556. Received July 13, 1974

Abstract: Pulsed FT proton magnetic resonance measurements and chemical shift analysis have been carried out in order to determine the dynamic solubilization site of the pyrene chromophore in cationic micellar solutions of pyrene, pyrene butyric acid (PBA), and pyrene sulfonic acid (PSA). Pyrene is solubilized in the interior of cetyltrimethyl ammonium bromide (CTAB) micelles while the pyrene chromophore of PBA and PSA is located in the outer core and surface region of the micelle, respectively. PSA and PBA in aqueous and micellar solutions were excited with 347.1-nm ruby laser light. The fluorescence lifetime of PSA is 62 nsec in water and 140 or 30 nsec in micellar solution of dodecyltrimethyl ammonium chloride (DTAC) or CTAB; for PBA the respective values are 140, 200, and 158 nsec. These results are explained in terms of stabilization of the excited singlet states of the probes by the micellar environment and quenching by Br^- counterions. For PBA the quenching efficiency of Br^- is much lower than for PSA due to the larger separation of the pyrene ring from the micellar Stern layer. The 347.1-nm laser photolysis of PSA and PBA in water also produces a large yield of hydrated electrons *via* a biphotonic photoionization process. In the case of PSA the photoionization is strongly inhibited by cationic micelles.

The structure and dynamics of organized multimolecular assemblies such as micelles or membranes have been explored by means of various photochemical methods. Fluorescent probes have been elegantly employed as sensors for the distinct microenvironment found in such biological macromolecules.² Probes suitable for these investigations usually display a selective affinity for a unique site on the macromolecule and reflect the nature of this environment in their emission properties. Thus the local polarity or viscosity may be inferred from quantum yield, emission lifetime, or the degree of polarization of the fluorescence. Similarly the kinetic analysis of fluorescence quenching reactions provides useful information about the permeability of bioaggregates with respect to ionic and nonionic quencher molecules.³⁻¹⁰

In previously reported laser photolysis studies of micelles and membrane vesicles³⁻⁷ pyrene was selected as the photoactive probe. The long-lived pyrene excited singlet state¹¹ may be used for the investigation of fluorescence quenching reactions at relatively small quencher concentrations. The relatively slow movement of pyrene within the macromolecule can also be studied.⁴ Due to its hydrophobic nature pyrene dissolves primarily in the unpolar interior of micelles or vesicles where it is randomly distributed. A more precise location of the pyrene chromophore can be achieved with derivatives such as pyrenebutyrate and pyrene sulfonate as the photoactive probes. It is reasonable to suppose that the anionic side groups of these amphiphiles associate with positively charged sites of biological macromolecules. Hence in aqueous solutions of cationic micelles such as cetyltrimethylammonium bromide (CTAB) or dodecyltrimethylammonium chloride (DTAC), a configuration is anticipated where the anionic side group is located in the Stern layer, with the hydrophobic pyrene chromophore protruding into the micellar palisade layer. Deeper penetration is expected to occur for pyrene butyric acid (PBA) than for pyrene sulfonic acid (PSA). Hence, the intriguing prospect consists of photochemically probing a narrow region within the outer core and surface of micelles. In the first part of this paper nmr investigations are described which assess the solubilization site of pyrene, PSA, and PBA in micellar solution. The nmr results are used in the second section to discuss fluores-

cence properties of the probes and to explain significant differences in their photochemical behavior in micellar and pure aqueous solutions.

Experimental Section

Apparatus. Laser photolysis experiments were carried out with a Korad frequency doubled, Q-switched ruby laser. The 347.1-nm laser pulse had a width of 15 nsec with an energy output of ~ 200 mJ. Transient absorption and fluorescence were detected by means of fast kinetic spectroscopy in the nanosecond to millisecond time domain. A detailed description of this technique has been given elsewhere.¹² An Aminco-Bowman spectrophotofluorometer was used for fluorescence measurements. Optical absorption studies were carried out on a Cary 14 spectrophotometer.

The ^1H nuclear magnetic resonance spectra were recorded on a Varian Associates A-60 A spectrometer. Some spectra were obtained at 100 MHz with a Varian XL-100 spectrometer using pulsed radiofrequency power and Fourier transform analysis. The free induction decay was accumulated and transformed with a 16K Nicolet TT-100 computer. All spectra were determined at ambient probe temperature (35°) on freshly prepared solutions in deuterium oxide contained in a Wilmad 5-mm coaxial capillary. A 30% solution of TMS in CDCl_3 was used as an external standard. The accuracy of the shifts are estimated to be ± 0.004 ppm. The reported chemical shifts are averages of 3-5 separate measurements.

Material. CTAB (Fluka, purum) and DTAC (Eastman Kodak) were purified by repeated recrystallization from ethanol-diethyl ether mixtures. 1-Pyrene butyric acid (Pfaltz & Bauer) and 1-pyrene sulfonic acid (Frinton) were used as supplied. Pyrene (Kodak) was passed through silica gel in cyclohexane solution and then recovered. Laboratory distilled water was redistilled from potassium permanganate. Deuterium oxide (Merck & Co., 99% D) was used as supplied.

Sample Preparation. An aliquot of a stock solution of pyrene or PBA in heptane or benzene was placed in a dry volumetric flask, and the solvent was evaporated with a stream of nitrogen. The precipitated solute is dispersed as a thin coating on the wall of the flask and can readily be resolubilized in a detergent solution by stirring the mixture for several hours. The samples were deoxygenated by bubbling with nitrogen for 15-30 min.

Results and Discussion

(1) Proton Nmr Investigations. A convenient and reliable means to assess the dynamic solubilization site of pyrene and its derivatives in micellar systems is provided by ^1H

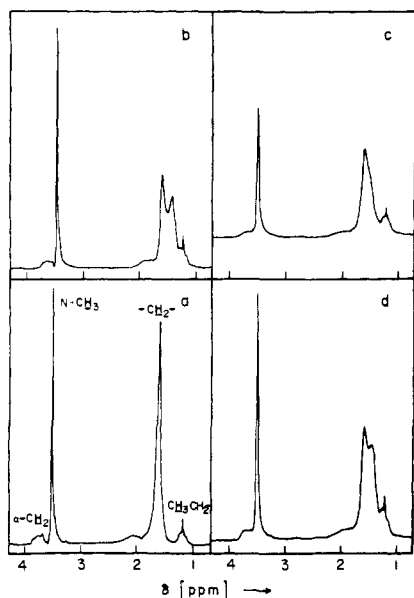


Figure 1. Proton nmr spectra of CTAB in solubilize free (a) solution and in the presence of pyrene (b), PSA (c), and PBA (d): CTAB = 0.1 *M*; solubilizates = 0.01 *M*.

Table I. Change in Chemical Shifts ($\Delta\delta$) of CTAB Protons for the Addition of Solubilizates in D_2O^a

Type of proton	$\Delta\delta^b$		
	Pyrene	PBA	PSA
N-(CH ₃) ₃	0.033	0.041	0.042
(CH ₂) _n	0.016	0.033	0.033
CH ₃ (CH ₂) _n	0.141 ^c	0.108 ^c	0.017

^a In ppm at 60 MHz and at $\sim 35^\circ$, relative to external TMS standard; [CTAB] = 0.1 *M*; [solubilizate] = 0.01 *M*. ^b $\Delta\delta$ = differences in chemical shifts of respective protons in CTAB solutions with and without solubilizate. ^c These values refer to differences in the chemical shift of the second split peak to the original position of CH₂ protons in solubilizate free CTAB solution (see Discussion).

nmr spectroscopy. The nmr spectrum of micellized CTAB is composed of four peaks corresponding to terminal methyl, methylene, α -methylene, and *N*-methyl proton resonances.¹³ These lines are usually upfield shifted upon solubilization of aromatic compounds since the aromatic ring gives a negative contribution to the local magnetic field encountered by neighboring protons. Thus by comparing nmr spectra of CTAB containing solubilized pyrene, PBA, and PSA with solubilizate free solutions it should be possible to determine the localization of the pyrene chromophore within the micellar assembly.

Interesting qualitative features concerning the interaction of these solubilizates with CTAB micelles are revealed in Figure 1, which shows ¹H nmr spectra of solutions containing 0.1 *M* CTAB and added 0.01 *M* pyrene, PBA, or PSA. The spectra were obtained by the pulsed FT nmr technique which is superior to conventional nmr with respect to resolution and signal-to-noise ratio. This technique makes it possible to obtain a clear resolution of the α -CH₂ multiplet in CTAB solutions (Figure 1a). Hitherto this was difficult to observe because of interference of the much stronger adjacent N-CH₃ resonance. The most prominent changes occur in the methylene resonances of the four solutions. Pyrene dramatically affects the CH₂ line by resolving it into two well-defined peaks of comparable size. Less pronounced splitting is caused by PBA and only broadening

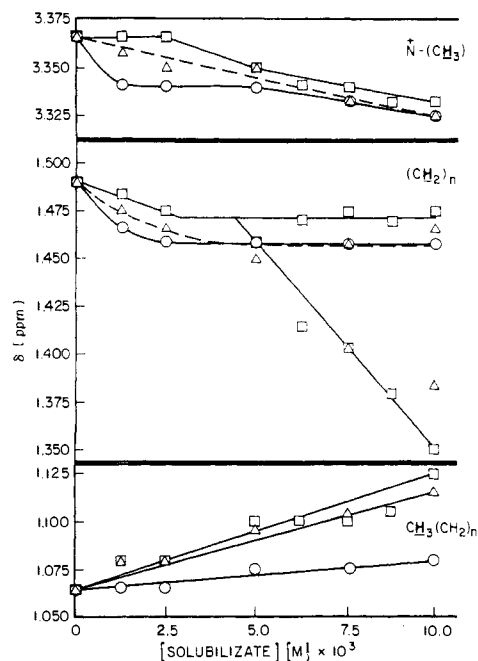


Figure 2. Chemical shifts of CTAB protons as functions of solubilizate concentration, in D_2O at 35° : Pyrene, O; PBA, Δ ; PSA, \square (CTAB = 0.1 *M*).

toward higher fields by PSA. Conversely PSA has a stronger influence on the α -CH₂ and N-CH₃ resonance than the other compounds. The N-CH₃ line width increases from pyrene to PSA solutions with an intermediate value for PBA. Similarly the α -multiplet is clearly separated from the N-CH₃ peak in the pyrene-CTAB spectrum while it is broadened and merges with the adjacent peak in the PBA and prominently in the PSA spectrum.

In order to quantitatively ascertain the effect of pyrene, PSA and PBA on the position of the CTAB resonances chemical shifts were determined at different solubilizate concentrations. These data are shown in Figure 2 while Table I summarizes the change in chemical shift $\Delta\delta$ obtained for a detergent-solubilizate mole ratio of 10:1. All three pyrene compounds cause a slight downfield shift of the methyl protons. The effect is very small, hardly exceeding the error limit in PSA solutions, and increases in the order PSA < PBA < pyrene. A similar effect is found for the shift of methylene protons. Here an initial slight upfield shift occurring at small solubilizate concentration is followed by peak splitting at pyrene and PBA concentrations larger than *ca.* 5×10^{-3} *M*. Further addition of solubilizate rapidly increases the separation of the two peaks, the split peak moving upfield while the other peak remains in its original position. $\Delta\delta$ (pyrene) is considerably larger than $\Delta\delta$ (PBA) as the shift of the split peak is more concentration dependent for the former solubilizate. The N-CH₃ line is shifted upfield by all three solutes with PSA solutions showing larger shifts than PBA or pyrene.

The above observations may be rationalized in terms of different solubilization sites of the pyrene ring in CTAB micellar solutions of pyrene, PSA, and PBA. Particular attention should be paid to the behavior of the methylene peak in the presence of solubilizate, in particular, the splitting caused by relatively small concentrations of pyrene and PBA. A similar phenomenon has been previously observed in CTAB solutions of tosylate;¹⁴ however, a higher solubilizate-detergent mole ratio was required to produce the effect. The concentration-dependent split peak may be assigned to methylene protons located in close proximity to the aromatic ring. It should be noted that the methylene

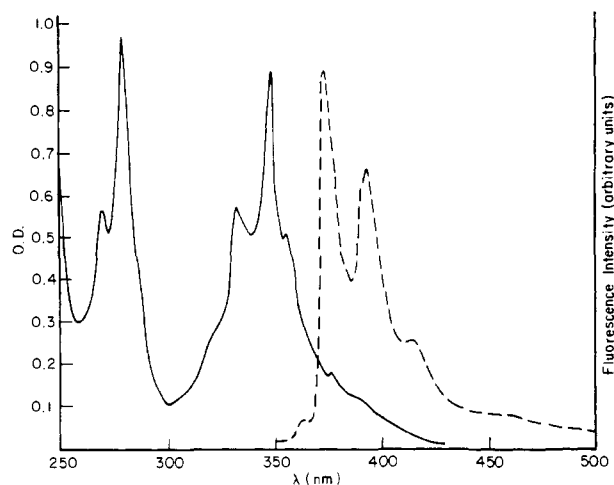


Figure 3. Absorption and fluorescence spectra of PSA ($4 \times 10^{-5} M$) in $0.1 M$ DTAC (λ_{excit} for fluorescence 347 nm).

peak includes only protons from inner CH_2 groups which are in the γ position or further away from the ammonium head groups. (The β - CH_2 resonance appears as a hump on the left side of the methylene peak.) The absence of splitting in the case of PSA solutions then implies that only inefficient contact exists between those inner methylene groups and the pyrene residue. This indicates that PSA is solubilized in the immediate surface region of a CTAB micelle. Pyrene as the other extreme produces a strong splitting effect which is indicative of frequent contact with inner methylene groups. This finding agrees with recent laser photolysis results⁴ which predict a random distribution of pyrene in the core region of CTAB micelles. Finally the splitting produced by PBA indicates location of the pyrene ring in an intermediate region of CTAB micelles: more deeply buried than PSA but with less access to inner CH_2 groups than pyrene.

The above interpretation is amplified by the chemical shift curves of the other resonances. PSA exerts maximum influence on the $\text{N}-\text{CH}_3$ line. Both replacement of water by PSA at the interface leading to a reduced polarity and also interaction with the aromatic ring may be responsible for the observed upfield shifts. Conversely, pyrene induces a maximum downfield shift of the terminal CH_3 signal. This effect may be interpreted as an increase in the separation of terminal CH_3 groups caused by the insertion of solubilize between the surfactant chain molecules. Here again the virtual absence of any change in the case of PSA is precluding its presence in the interior of a CTAB micelle.

It may be concluded that a transition of the pyrene chromophore from the interior toward the surface of a CTAB micelle occurs as the solubilize changes from pyrene to PBA and PSA as would be expected if the negative side group of the pyrene derivative was associated with positive charges in the micellar Stern layer. This information may now be used in the analysis of photochemical data obtained with the same systems.

(2) **Photochemical Studies. (a) Fluorescence Studies of PSA Solutions.** The absorption spectrum of PSA in an aqueous micellar solution of DTAC is shown in Figure 3. It is similar to the spectrum published for pyrene.¹⁵ A conspicuous shift was noted in the position of the 0,0-1,1 transition which is located at 334 nm for pyrene in cyclohexane. The corresponding bands in PSA in water, and DTAC, or CTAB are at 346.5 and 348.5 nm , respectively. The molar extinction coefficient for this transition in PSA solutions was found to be 2.25×10^4 , which is comparable to literature values for the same absorption band in pyrene.¹⁶ This

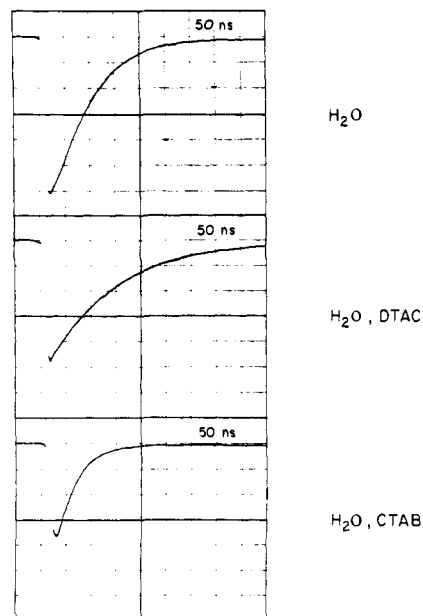


Figure 4. Decay of PSA fluorescence (ordinate: relative fluorescence intensity) in aqueous and in micellar (in $0.1 M$ DTAC and in $0.02 M$ CTAB) solutions; $\lambda 400 \text{ nm}$.

strong absorption in the vicinity of the laser line at 347.1 nm makes it possible to excite PSA at low concentrations.

The fluorescence spectrum of PSA in micellar DTAC solutions, Figure 3, shows two peaks at $\lambda 374$ and 394 nm and a shoulder at $\lambda \sim 415 \text{ nm}$, and is almost identical with the emission spectrum in aqueous solution.^{17,18} Laser photolysis experiments give the oscilloscope traces shown in Figure 4. The traces show the PSA fluorescence decay in various solutions. In deaerated water a fluorescence lifetime $\tau_f = 62 \text{ nsec}$ is obtained which is slightly longer than the previously published value $\tau_f = 50 \text{ nsec}$.¹⁸ In the presence of DTAC micelles τ_f increases by more than a factor of 2 to 140 nsec . However the lifetime of PSA fluorescence is much shorter in CTAB micellar solutions where a value $\tau_f = 30 \text{ nsec}$ is measured. The significant increase in the PSA fluorescence lifetime in DTAC micelles is connected with the nature of the interaction of the PSA excited singlet state with its immediate environment in the micellar surface region. It is reminiscent of the fluorescence behavior displayed by *N*-arylamino-naphthalene sulfonates. In this class of fluorescent probes the fluorescence lifetime and quantum yield increase sharply with decreasing polarity of the medium.² In particular a strong enhancement of fluorescence has been observed when these probes are absorbed on the surface of cationic micelles,^{19,20} where the local dielectric constant may have a value of *ca.* 30.²¹ These phenomena have been attributed to solvent relaxation during the lifetime of the excited states.^{2d} This mechanism is supported by the observation that the fluorescence maximum shifts to a longer wavelength with increasing polarity of the environment. In the case of PSA solutions in micellar DTAC, the increase in the fluorescence lifetime is not accompanied by a shift in the fluorescence maximum. This indicates that solvent relaxation is unlikely to account for the observed effect. Presumably the stabilization of the PSA excited singlet state by the micellar microenvironment is caused by a medium effect on the interaction of the sulfonate side group with the aromatic ring system. It has been suggested previously²² that the shorter fluorescence lifetimes of pyrene derivatives, as compared to pyrene ($\tau_f = 450 \text{ nsec}$),¹¹ result from conjugation of the side groups with the π -electron system. As PSA is solubilized close to the surface of a DTAC micelle it

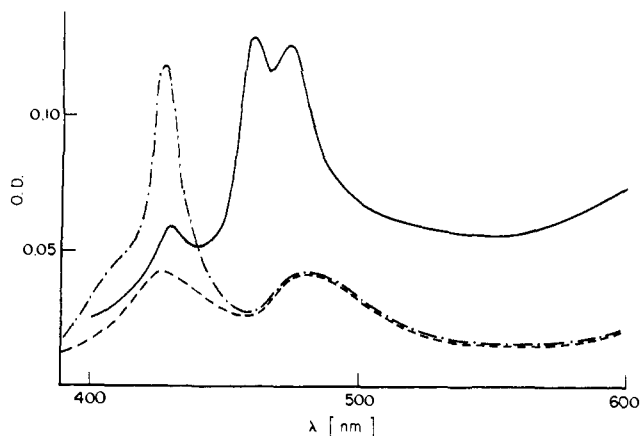


Figure 5. Transient absorption spectra obtained by 347.1 nm laser photolysis of $2 \times 10^{-5} M$ PSA in water (—), in $0.02 M$ CTAB (- - -), and $0.1 M$ DTAC (- · -) solutions. Spectra obtained immediately after the laser pulse.

encounters positive charges that withdraw electron density from the sulfonate group. In this configuration the extent of conjugation with the pyrene ring may be reduced. This would explain both the increase in fluorescence lifetime and red shift of the absorption maximum.

The relatively short fluorescence lifetime of PSA in CTAB micellar solution can be readily understood in terms of quenching of the excited state by the bromide counterions. Similar effects have been reported for naphthalene,^{20,23} anthracene,²⁴ and pyrene⁴ solubilized in CTAB micelles. In a pure aqueous phase the quenching of PSA excited states by Br^- is relatively inefficient, hence relatively high bromide concentrations are required to produce a decrease of the PSA fluorescence lifetime. The quenching rate constant determined at 0.2 and $0.4 M$ NaBr is $5 \times 10^7 M^{-1} \text{sec}^{-1}$.

The quenching effect is much more pronounced in CTAB solution due to the fact that PSA is located close to the micellar Stern layer where the Br^- concentration is extremely high. An estimate for the Br^- concentration in the Stern layer of a CTAB micelle can be made from a theoretical treatment²⁵ which takes into account the finite size of the counterions and of the ionic head groups. Using a value of 4.6 \AA for the thickness of the Stern layer one calculates by means of eq 4 in ref 25 $[\text{Br}^-]_s = 6.6 M$. An alternative approach is to divide the number of Br^- ions bound to one micelle²⁶ by the total volume of the Stern layer; it gives a somewhat lower value of $3.1 M$.

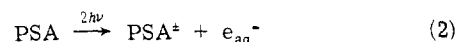
These two estimates for the Br^- counterion concentration in the Stern layer of a CTAB micelle may be compared with the effective bromide concentration in the vicinity of a PSA probe. This can be calculated from the fluorescence lifetimes τ_1 and τ_2 observed in micellar CTAB and DTAC solutions, respectively.

$$[\text{Br}^-]_{\text{eff}} = 1/k((1/\tau_1) - (1/\tau_2)) \quad (1)$$

Assuming the same rate constant k for the quenching of PSA excited states by bromide ions in aqueous and micellar environment, one obtains $[\text{Br}^-]_{\text{eff}} = 0.52 M$. Although this value is lower than the theoretical estimates it indicates that the pyrene chromophore in micellar PSA solution encounters a high local Br^- concentration and is probably located in the immediate surface region of the CTAB micelle.

(b) **Transient Absorption Studies in PSA Solutions.** In order to obtain a complete picture of the photochemical events occurring during the laser photolysis of PSA solutions it is necessary, in addition to the fluorescence studies,

to investigate the possible formation and behavior of non-fluorescent transitory species. The identification of these species can be made on the basis of their characteristic absorption spectra, using the technique of fast kinetic spectroscopy. In Figure 5 the change in the optical density immediately after the laser pulse is plotted as a function of wavelength for aqueous and micellar solutions of PSA. In a neat aqueous solution the transitory spectrum shows three distinct peaks and a broad band rising toward the red. The latter absorption is removed by typical electron scavengers such as N_2O and nitrate and is thus attributed to the hydrated electron. The peaks at 427 and 460 nm can be assigned to the PSA triplet state and PSA zwitterion, respectively. These assignments are made by examining the behavior of the absorption maxima to additives such as OH^- and O_2 which selectively react with the zwitterions or triplets. The absorption maximum at 473 nm is due to PSA excited singlet states, as the decay kinetics match those of the fluorescence decay. The formation of hydrated electrons and PSA zwitterions in the laser photolysis of aqueous PSA solutions is a biphotonic photoionization.



A biphotonic assignment is given to this process as the yield of hydrated electrons is proportional to the square of the intensity of the laser light. The parent radical ions PSA^\pm may be viewed as zwitterions with the negative charge located at the sulfonate group and the positive charge within the pyrene aromatic ring. Such a structure is suggested by the similarity of the PSA^\pm absorption spectrum with that of pyrene positive ions.^{27,28}

While the photoionization of PSA occurs with a large cross section in aqueous solution it is almost completely suppressed if PSA is adsorbed at the surface of cationic micelles. This is apparent from the transitory spectra obtained from the laser photolysis of PSA in micellar DTAC and CTAB solutions; data are shown in Figure 5. Both spectra lack the pronounced peak of the PSA^\pm zwitterions at 460 nm and the hydrated electron absorption at longer wavelengths. Just as the PSA fluorescence lifetime is enhanced in micellar solution, the inhibition of the photoionization process in these systems may also be caused by the local electrostatic field in the micellar surface region. The electrostatic field will withdraw electron density from the PSA molecule. It is unlikely that the observed effect is due to immediate retrapping of photoejected electrons in the micellar potential field, followed by rapid recombination with the parent ion. Earlier investigations with pyrene solutions have shown that the photoejected electrons have considerable excess energy and can escape the field of their parent micelles.²⁹ Returning to Figure 5 one also notices a striking enhancement of the triplet absorption peak at 427 nm as one goes from DTAC to CTAB micellar solutions of PSA. This pronounced increase in the triplet yield is due to the quenching of PSA singlet excited states with bromide ions in the Stern layer of CTAB micelles. This shows that the quenching of the PSA fluorescence by Br^- counterions results in the promotion of intersystem crossing by a heavy atom effect. A different mechanism has been suggested for the quenching of naphthalene excited singlets by Br^- ions.¹⁴ Presumably the latter reaction is a nucleophilic addition of Br^- to the naphthalene aromatic ring.

It is instructive to compare the kinetics of the PSA triplet decay in aqueous and micellar CTAB solutions. In water the triplet state decays mainly *via* triplet-triplet annihilation. This bimolecular process occurs with a diffusion-controlled rate constant of *ca.* $10^{10} M^{-1} \text{sec}^{-1}$. As the laser

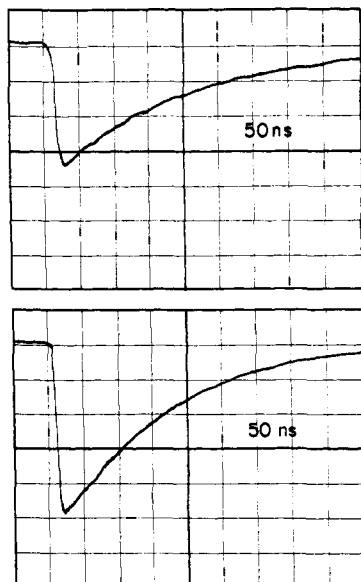


Figure 6. Decay of PBA ($2 \times 10^{-5} M$) fluorescence in 0.1 M DTAC (upper trace) and in 0.02 M CTAB (lower trace) solutions: λ 400 nm.

pulse produces a concentration of PSA triplets between $2 \times 10^{-6} M$ and $10^{-5} M$, then the first half-lifetime of the triplet decay is 10–50 μsec . In micellar solution a much longer triplet decay time of 10–20 msec is observed indicating that CTAB micelles stabilize the PSA triplet state. This effect can be readily explained in terms of micellar inhibition of the triplet annihilation process. The encounters between PSA triplet states which are associated with CTAB micelles are prevented by: the slow diffusion of the micellar carriers, the electrostatic repulsion between the micelles, and protection by surfactant molecules adjacent to the pyrene chromophore in the palisade layer. The slow decay of the triplets in micellar solution is also indicative of a strong binding of PSA to CTAB micelles. As the triplet decay curve is smooth without an initial fast component, then the PSA ions must be almost quantitatively associated with the micelles. The dissociation rate is relatively slow as indicated by the long lifetime of the triplets. An upper limit for the dissociation rate constant may be estimated⁵ as $5 \times 10^{-2} \text{sec}^{-1}$.

(c) Fluorescence and Transient Absorptions Studies of PBA Solutions. The absorption and emission spectra of pyrene butyric acid in various solutions have been reported previously.^{30,31} In solutions of DTAC the position of the 0,0–1,1 transition is at 345.3 nm compared to 343 nm in water.³⁰ The kinetics of the fluorescence decay in water, DTAC, and CTAB solutions were investigated using the laser photolysis technique. In water the fluorescence lifetime was found to be 140 nsec which agrees well with the literature value.²² Oscilloscope traces showing the PBA fluorescence decay in micellar DTAC and CTAB solution are presented in Figure 6. In micellar DTAC solutions the fluorescence lifetime is 200 nsec and is similar to values found for PBA in bovine serum albumin³⁰ and 1,2-propanediol solutions.²² If CTAB is used, the lifetime decreases to 158 nsec. This contrasts sharply to the results obtained with PSA solutions, where the fluorescence lifetime in the CTAB system is much shorter than in the DTAC system. Apparently the PBA excited states are less efficiently quenched by the Br^- counterions of the CTAB micelles than PSA excited states. A quantitative measure of the quenching efficiency is given by the difference of the reciprocal half-lifetimes in CTAB (τ_1) and DTAC (τ_2) solutions (see eq 3). One calculates $k_e = 2.1 \times 10^6 \text{sec}^{-1}$ for PBA and $k_e = 2.6$

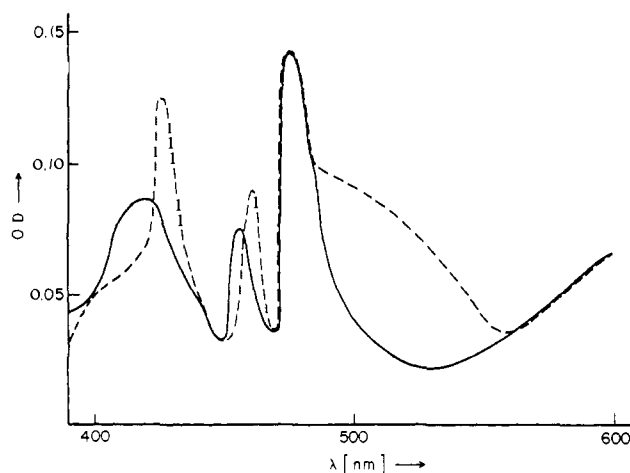


Figure 7. Transient absorption spectra obtained by 347.1-nm laser photolysis of PBA ($2 \times 10^{-5} M$) in water (pH 11) (—) and in 0.02 M CTAB (---) solutions. Spectra obtained immediately after the pulse.

$\times 10^7 \text{sec}^{-1}$ for PSA. For pyrene solutions $\tau_1 = 150 \text{nsec}^5$ and τ_2 was determined as 353 nsec, hence $k_e = 3.8 \times 10^6 \text{sec}^{-1}$.

$$k_e = (1/\tau_1) - (1/\tau_2) \quad (3)$$

A rationale for the difference in the quenching efficiencies k_e is provided by a consideration of the site of the pyrene chromophore in a CTAB micelle. It was noted earlier, in the nmr section, that the pyrene ring of PBA is located within the outer core region of the micelle. The restricted motility of the butyrate side chain interferes with the movement of the pyrene chromophore toward the Stern Layer where the Br^- ions are located. Hence the efficiency of the Br^- quenching reaction is low. Pyrene, on the other hand, is quenched more efficiently by the counterions since it can move freely through the micellar interior. In the case of PSA the chromophore is located adjacent to the Stern layer which leads to frequent encounters with Br^- ions and therefore very efficient quenching. In homogeneous solution all three probes react with Br^- ions with nearly the same rate constant. The pronounced difference in the quenching efficiencies cannot be due to a variation in the quenching rate constant of these probes.

The fluorescence kinetics of PSA and PBA in micellar CTAB solution give some measure of the degree of roughness of the micellar surface which is disputed in the literature.^{32,33} If the fluctuations in the radial position of the ammonium head groups were of the order of the length of a butyrate chain ($\sim 4\text{--}5 \text{Å}$), then the effective quenching constant k_e should be the same for PSA and PBA. Both probes would encounter Br^- counterions with a similar probability in this geometry. However, the observed large difference between k_e for PSA and PBA indicates that any undulations of the micellar surface are considerably less than 4–5 Å .

Finally Figure 7 shows the absorption spectrum of transitory species formed during the laser photolysis of PBA solutions. The transitory spectrum obtained immediately after the laser pulse in aqueous medium resembles that of PSA in Figure 5. The characteristic absorption band of hydrated electrons in the red and the absorption maximum of the PBA zwitterions at 460 nm are evident. The formation of these ions again occurs *via* biphotonic photoionization. The peaks at 430 and 470 nm can be readily assigned to PBA triplets and singlets, respectively. The transitory spectrum obtained in CTAB micellar solution of PBA shows features

similar to the spectrum in water. The absorption maxima of PBA triplets and zwitterions are slightly red shifted compared to aqueous solutions and a relatively small increase in the height of the triplet peak is observed.

The similarity of the transitory spectra obtained in the laser photolysis of aqueous and micellar PBA solutions stands in sharp contrast to the drastic difference of these spectra in PSA solutions. In the PSA system micellar inhibition of the photoionization process, and strong enhancement of the triplet absorption peak, were observed. The latter effect can be readily understood in terms of more efficient quenching of PSA singlet excited states than those of PBA by Br^- counterions leading to a higher triplet yield in CTAB micellar solutions. The fact that photoionization can occur in micellar PBA solutions but not in PSA solutions implies that photoejection of electrons is possible when the pyrene chromophore is located away from the surface of the cationic micelle. The data confirm the earlier conclusion, that the microenvironment of the pyrene chromophore in PSA solutions, and in particular the local electrostatic field in the micellar Stern layer, plays an important role in the inhibition of the photoionization process.

Conclusion

The nmr data and the kinetic analysis of fluorescence decay curves both demonstrate that the solubilizations of PSA and PBA lead to configurations where the anionic side groups of the probes are associated with positive surface charges of the micelle. The hydrophobic residue meanwhile protrudes into the unpolar micellar interior. The data give useful hints regarding the interaction of these probes with biological macromolecules such as proteins and membranes. Thus the pyrene chromophore of PBA and PSA is expected to reside in an unpolar microenvironment in the vicinity of positively charged sites of the bioaggregate. Another important feature is the fact that certain photoreactions, such as the photoionization process, may be prevented by the presence of a charged interface in the neighborhood of the chromophore. This has bearing on photoreactions in physiological solutions, where charged interfaces with potential gradients are frequently encountered.

Acknowledgment is made to the donors of the Petroleum Research Fund, administered by the American Chemical Society, for partial support of this research.

References and Notes

- (1) The Radiation Laboratory is operated by the University of Notre Dame under contract with the U. S. Atomic Energy Commission. This is AEC Document No. COO-38-963.
- (2) (a) G. Weber, *Annu. Rev. Biophys. Bioeng.*, **1**, 553 (1972); (b) G. Weber and D. J. R. Laurence, *Biochem. J.*, **56**, 31 (1954); (c) G. K. Radda, "Current Topics In Bioenergetics," Vol. 4, Academic Press, New York N.Y., 1971, p 81; (d) L. Brand and J. R. Gohlke, *Ann. Rev. Biochem.*, **41**, 843 (1972); (e) G. M. Edelman and W. O. McClure, *Accounts Chem. Res.*, **1**, 65 (1968); (f) A. S. Wagonner and L. Stryer, *Proc. Nat. Acad. Sci. U. S.*, **67**, 579 (1970).
- (3) S. C. Wallace and J. K. Thomas, *Radiat. Res.*, **54**, 49 (1973).
- (4) M. Grätzel and J. K. Thomas, *J. Amer. Chem. Soc.*, **95**, 6885 (1973).
- (5) P. P. Infelta, M. Grätzel, and J. K. Thomas, *J. Phys. Chem.*, **78**, 190 (1974).
- (6) S. Cheng, J. K. Thomas, and C. F. Kulpa, *Biochemistry*, **13**, 1135 (1974).
- (7) M. Chen, M. Grätzel, and J. K. Thomas, *Chem. Phys. Lett.*, **24**, 65 (1974).
- (8) (a) J. R. Lakowicz and G. Weber, *Biochemistry*, **12**, 4161 (1973); (b) *ibid.*, **12**, 4171 (1973).
- (9) (a) H. J. Pownall and L. C. Smith, *ibid.*, **13**, 2590 (1974); (b) *ibid.*, **13**, 2594 (1974).
- (10) H. J. Pownall and L. C. Smith, *J. Amer. Chem. Soc.*, **95**, 3136 (1973).
- (11) J. B. Birks and H. Munro, *Progr. React. Kinet.*, **4**, 239 (1967).
- (12) R. McNeil, J. T. Richards, and J. K. Thomas, *J. Phys. Chem.*, **74**, 2290 (1970).
- (13) J. G. Erikson and G. Gillberg, *Acta Chem. Scand.*, **20**, 2019 (1966).
- (14) (a) C. A. Bunton, "Reaction Kinetics in Micelles," E. H. Cordes, Ed., Plenum Press, New York, N.Y., 1973, p 89; (b) C. A. Bunton, M. J. Minch, J. Hidalgo, and L. Sepulveda, *J. Amer. Chem. Soc.*, **95**, 3262 (1973).
- (15) H. H. Jaffe and M. Orchin, "Theory and Applications of Ultraviolet Spectroscopy," Wiley, New York, N.Y., 1962, p 334.
- (16) I. B. Berlimann, "Fluorescence Spectra of Aromatic Molecules," Academic Press, New York, N.Y., 1971.
- (17) E. Döller, *Z. Phys. Chem. (Frankfurt am Main)*, **31**, 274 (1962).
- (18) J. R. Brocklehurst, R. B. Freedmann, D. J. Hancock, and G. K. Radda, *Biochem. J.*, **116**, 721 (1970).
- (19) B. Rubalcava, D. M. deMunoz, and C. Gittler, *Biochemistry*, **8**, 2742 (1969).
- (20) R. R. Hautala, N. E. Schore, and N. J. Turro, *J. Amer. Chem. Soc.*, **95**, 5508 (1973).
- (21) A. Ray and P. Mukerjee, *J. Phys. Chem.*, **70**, 2138 (1966).
- (22) R. D. Spencer, W. M. Vaughan, and G. Weber, "Molecular Luminescence," E. C. Lim, Ed., W. A. Benjamin, New York, N.Y., 1969, p 607.
- (23) R. R. Hautala and N. J. Turro, *Mol. Photochem.*, **4**, 595 (1972).
- (24) L. K. Patterson and E. Viel, *J. Phys. Chem.*, **77**, 1191 (1973).
- (25) D. Stigter, *J. Phys. Chem.*, **68**, 3603 (1964).
- (26) W. K. Mathews, J. W. Larsen, and M. T. Pikal, *Tetrahedron Lett.*, 513 (1972).
- (27) K. H. Grellmann and A. R. Watkins, *J. Amer. Chem. Soc.*, **95**, 983 (1973).
- (28) J. T. Richards, G. West, and J. K. Thomas, *J. Phys. Chem.*, **74**, 4137 (1970).
- (29) S. C. Wallace, M. Grätzel, and J. K. Thomas, *Chem. Phys. Lett.*, **23**, 359 (1973).
- (30) W. M. Vaughan and G. Weber, *Biochemistry*, **9**, 464 (1970).
- (31) J. A. Knopp and G. Weber, *J. Biol. Chem.*, **244**, 6309 (1969).
- (32) P. Mukerjee, *Advan. Colloid Interface Sci.*, **1**, 241 (1967).
- (33) D. Stigter and K. J. Mysels, *J. Phys. Chem.*, **59**, 45 (1955).